

## Observation of Two-Dimensional Dynamic Localization of Light

Alexander Szameit,<sup>1</sup> Ivan L. Garanovich,<sup>2</sup> Matthias Heinrich,<sup>3</sup> Andrey A. Sukhorukov,<sup>2</sup> Felix Dreisow,<sup>3</sup> Thomas Pertsch,<sup>3</sup> Stefan Nolte,<sup>3</sup> Andreas Tünnermann,<sup>3</sup> Stefano Longhi,<sup>4</sup> and Yuri S. Kivshar<sup>2</sup>

<sup>1</sup>*Solid State Institute and Physics Department, Technion, 32000 Haifa, Israel*

<sup>2</sup>*Nonlinear Physics Centre and Centre for Ultra-high Bandwidth Devices for Optical Systems (CUDOS), Research School of Physics and Engineering, Australian National University, Canberra, ACT 0200, Australia*

<sup>3</sup>*Institute of Applied Physics, Friedrich-Schiller-University Jena, Max-Wien-Platz 1, 07743 Jena, Germany*

<sup>4</sup>*Dipartimento di Fisica, Politecnico di Milano, I-20133 Milano, Italy*

(Received 4 February 2010; revised manuscript received 5 May 2010; published 1 June 2010)

We report on the first experimental observation of dynamic localization of light in two-dimensional photonic lattices. We demonstrate suppression of beam diffraction in hexagonal lattices created by weakly coupled waveguides with axis bending. We also reveal that this effect is strongly related to dynamic localization in zigzag waveguide arrays with next-nearest neighboring interactions.

DOI: 10.1103/PhysRevLett.104.223903

PACS numbers: 42.25.Fx, 42.82.Et

Because of the stunning correspondence between quantum mechanics and optics in waveguides, in the past few years many quantum-particle phenomena have been translated into an optical analogue, where the experimental accessibility is much simpler [1]. In this vein, a number of fundamental concepts such as the quantum Zeno effect [2] and coherent destruction of tunneling [3], atomic and molecular dynamics such as Rabi oscillations [4] or the non-Markovian decay of an isolated state into a continuum [5], and solid state phenomena like surface waves [6,7] and Anderson localization [8–13] have been experimentally demonstrated by employing an optics platform. Particular attention was devoted to the visualization of photonic analogues of coherent transport phenomena in crystals, such as Bloch oscillations [14–16], Zener tunneling [17], quasi-Bloch oscillations [18], and dynamic localization effect [19,20]. Albeit such phenomena have been also observed in several other physical systems, including cold atoms or Bose-Einstein condensates in accelerated optical lattices [21,22] and acoustical waves in layered media [23], most of the previous experimental studies were limited to the consideration of the coherent transport in one-dimensional geometries.

On the other hand, coherent transport in multidimensional lattices is generally strongly affected by lattice geometry, and it may show new effects with no counterpart in one-dimensional lattices. For instance, the motion of a two-dimensional Bloch particle under a dc driving field undergoes complex Lissajous-type trajectories, and anisotropic Zener tunneling occurs in the high-field regime. Similarly to Bloch oscillations, coherent transport in ac fields and dynamic localization are also affected by the effects of dimensionality and geometry of the lattice [24]. In this work we use the term “dynamic localization” (DL) in the sense in which it was originally introduced by Dunlap and Kenkre [24]. DL refers to the suppression of broadening of a particle wave packet during its motion in a

periodic potential under the action of an externally applied ac electric field [24–26], which is reminiscent of the self-collimation effect in photonic crystals [27]. This kind of localization is thus conceptually very different from other forms of localization, like Anderson localization [9,11–13] or localization in the periodically kicked quantum rotator problem [28]. DL was observed for cold atoms and Bose-Einstein condensates in one-dimensional optical lattices [29,30]. DL for optical wave packets has been recently observed in one-dimensional arrays of periodically curved waveguides, where a change of the waveguide curvature mimics the effects of an ac driving field [19,20]. In multidimensional lattices, application of suitable ac fields enables one to engineer the effective geometry and even dimensionality of the lattice [24,31]. For instance, an effectively one-dimensional wave packet spreading in a two-dimensional lattice was recently demonstrated [32] and explained as a partial DL resonance. Coherent control of matter waves in multidimensional lattices was also reported [33]. However, experimental realization of a complete suppression of wave packet broadening via the two-dimensional DL effect is still lacking.

In this Letter we report on the direct experimental observation of DL effect in two-dimensional periodic systems. This effect is registered as a strong suppression of two-dimensional diffraction and beam broadening in a hexagonal lattice created by periodically curved optical waveguides. We further demonstrate DL in zigzag-type waveguide arrays, and reveal that this phenomenon is strongly related to DL in quasi-one-dimensional lattices with next-nearest-neighboring coupling between the sites.

In our setting the waveguides are periodically bent in the ( $x$ - $z$ ) plane along the propagation direction  $z$ , which is expressed mathematically through the transverse shift of the waveguides  $x_0(z)$ . We define the complex beam envelope function  $\Psi(x, y, z)$  in the local coordinate system (moving with the lattice). Then, the beam dynamics can

be described by the Schrödinger-type equation [1]

$$i\lambda \frac{\partial \Psi}{\partial z} = - \left[ \frac{\lambda^2}{2n_0} \nabla_{\perp}^2 + \Delta n(x, y) - n_0 \ddot{x}_0(z)x \right] \Psi, \quad (1)$$

where  $\lambda = \lambda/2\pi$  is the reduced wavelength,  $n_0$  is the bulk refractive index,  $\Delta n(x, y)$  is the transverse refractive index variation caused by the waveguides, and the dot stands for the derivative in  $z$ . There is an evident similarity between Eq. (1) and the quantum mechanical Schrödinger equation for a nonrelativistic charged particle of mass  $m$  and charge  $q$  under the action of an external time-varying electric field, when one replaces the spatial coordinate  $z$  with time  $t$ , the reduced wavelength  $\lambda$  with the reduced Planck's constant  $\hbar$ , the refractive index  $n_0$  with the particle mass  $m$ , the optical potential  $\Delta n(x, y)$  with the quantum potential  $-V(x, y)$ , and the array bending  $n_0 \ddot{x}_0(z)$  with the external force  $-q\mathcal{E}(t)$  caused by the driving electric field  $\mathcal{E}(t)$ .

Light transport in the lattice can be approximately described by a tight-binding analysis of Eq. (1), where the total electric field envelope  $\Psi(x, y, z)$  is represented [31] as a superposition of the modes  $\Psi_0(x, y)$  of the individual waveguides numbered as  $n, m$ ,  $\Psi(x, y, z) \approx \sum_{n,m} E_{n,m}(z) \Psi_0[x - x_{n,m}, y, z] \exp[-i\omega \dot{x}_0(z)x_{n,m}/d]$ , where  $x_{n,m}$  are the waveguide coordinates, and for a hexagonal lattice shown schematically in Fig. 1(a)  $x_{n,m} = (n + m/2)d$ ,  $d$  is the waveguide spacing, and  $\omega = 2\pi n_0 d/\lambda$  is the dimensionless frequency. We take into account coupling between the modes of nearest wave-

guides, and obtain the resulting coupled-mode equations in the following form [31]:

$$i \frac{dE_{n,m}}{dz} = -C_1^* E_{n-1,m} - C_1 E_{n+1,m} - C_2^* E_{n,m-1} - C_2 E_{n,m+1} - C_3^* E_{n-1,m+1} - C_3 E_{n+1,m-1}, \quad (2)$$

where  $C_1 = C \exp[-i\omega \dot{x}_0(z)]$  and  $C_2 = C_3 = C \exp[-i\omega \dot{x}_0(z)/2]$  are the coupling coefficients between the neighboring waveguides [Fig. 1(a)], which phase is modified due to bending, and asterisk stands for the complex conjugation. The real-valued coefficient  $C$  defines the coupling strength and characterizes the diffraction rate in a straight hexagonal waveguide array with  $x_0 \equiv 0$ .

We have predicted recently [31] that a complete two-dimensional DL for both transverse dimensions can be realized for a special class of bending profiles, consisting of alternating straight and sinusoidal segments in each bending period  $L$ ,

$$x_0(z) = \begin{cases} 0, & \text{if } 0 \leq z \leq z_0, \\ A \{ \cos[\frac{2\pi(z-z_0)}{L-z_0}] - 1 \}, & \text{if } z_0 \leq z \leq L, \end{cases} \quad (3)$$

provided that the bending parameters satisfy the conditions  $z_0 = [1 - 1/J_0(\xi)]^{-1}L$  and  $A = -z_0 \xi / \pi \omega J_0(\xi)$ , where  $\xi \approx 2.61$  is defined by the equation  $J_0(\xi) = J_0(2\xi)$  and  $J_0$  is the Bessel function. The resulting waveguide bending profile which corresponds to our experimental samples is shown in Fig. 1(b).

In order to visually demonstrate the difference between the usual beam diffraction and beam dynamics in the regime of dynamic localization, we quantify the rate of beam spreading with the values of the participation ratio, defined as  $PR = \ln[(\sum_{n,m} |E_{n,m}|^2)^2 / \sum_{n,m} |E_{n,m}|^4]$ . We use the discrete Eq. (2) to compute numerically participation ratios, and show in Fig. 1(c) the characteristic dependencies  $PR(z)$  for beams propagating in straight (dashed line) and curved lattices where the condition for DL is satisfied (solid line). In these examples, we have considered input excitation of a single waveguide. We see that in the straight lattice continuous diffraction-induced broadening of the beam occurs, whereas in the curved lattice beam size experiences periodic oscillations and full refocusing after each waveguide bending period  $L$  as a result of the two-dimensional dynamic localization.

In order to observe DL experimentally, we fabricated two-dimensional hexagonal waveguide arrays using the direct femtosecond laser-writing technique in fused silica glass [34]. When ultrashort laser pulses are focused into the bulk silica, the density is locally increased. Accordingly, the refractive index is locally increased in the exposed regions, and these act as optical waveguides. We move the sample continuously with respect to the beam to inscribe curved waveguides of the required shape. Our samples contain one full bending period with  $L = 25$  mm, and the spacing between neighboring waveguides

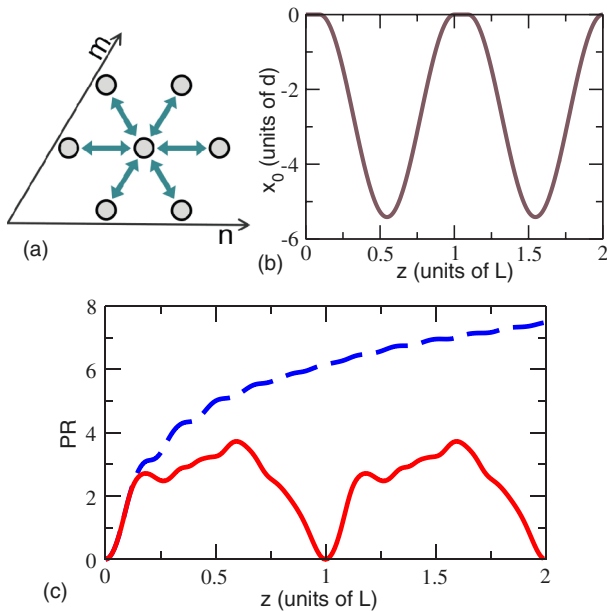


FIG. 1 (color online). (a) Sketch of the couplings in a hexagonal lattice. (b) Periodic waveguide bending profile. (c) Numerically calculated participation ratios for the lattices created by straight (dashed) and curved (solid) waveguides. Parameters match the measured characteristics of the experimental samples.

is  $d = 22 \mu\text{m}$ . Samples have hexagon-shaped boundaries with 5 waveguides at each facet [see Fig. 2(a)]. To characterize the arrays, we launch cw laser light at the wavelength  $\lambda = 633 \text{ nm}$  into the central waveguide of the samples. Experimentally measured output beam profile for the straight sample is shown in Fig. 2(a), where strong beam diffraction is recorded. One can notice that light already hits the sample boundaries because of the finite number of the waveguides in the array. In contrast, in the curved sample the full suppression of the output beam diffraction in all transverse directions is clearly visible [Fig. 2(c)]. Experimentally observed diffraction patterns are in a good agreement with the output profiles calculated by numerical integration of Eq. (2). We choose the coupling coefficient  $C = 0.165 \text{ mm}^{-1}$  to match the diffraction pattern at the output of the straight array [cf. Figs. 2(a) and 2(b)], and then confirm that the DL regime is present under such conditions [cf. Figs. 2(c) and 2(d)]. Our simulations indicate that the diffraction is strongly reduced in the curved samples, such that the light does not hit the sample boundaries and DL is not affected by the finite array size in our experiments. Importantly, two-dimensional DL is achieved in our experiments using purely one-dimensional lattice modulation [Eq. (3)] in the  $(x, z)$  plane.

A similar DL effect can also be observed in zigzag shaped lattices [35], which are described by Eq. (2) with  $m$  taking values  $m = 1, 2$  [see Fig. 3(a)]. Interestingly, such zigzag lattices can be considered as quasi-one-dimensional lattices with the next-nearest-neighbor lattice site interaction [36] if we number all lattice sites with a single index  $n$  according to their position along  $n$  axis [Fig. 3(a)]. Then the coupled-mode equations for the modal amplitudes at

the various waveguides read

$$i \frac{dE_n}{dz} = -C_2^* E_{n-1} - C_2 E_{n+1} - C_1^* E_{n-2} - C_1 E_{n+2}, \quad (4)$$

where the values of  $C_1$  and  $C_2$  play the role of the coupling strengths between the nearest and next-nearest neighbors. We further note that the DL regime can be realized in the periodically curved zigzag lattice with exactly the same waveguide bending profile as was used for the hexagonal lattice. The equivalence between the two-dimensional diffraction suppression in the hexagonal and quasi-one-dimensional zigzag lattices can be ascribed to the topological similarity of the unit cells in both cases [cf. Figs. 1(a) and 3(a)]. Participation ratios computed numerically for infinite zigzag arrays by solving Eq. (4) are shown in Fig. 3(b). Similar to the case of the hexagonal array, light beam experiences periodic refocusing in the curved zigzag array in the DL regime [Fig. 3(b), solid curve], in contrast to the diffraction broadening in the straight array [Fig. 3(b), dashed curve].

To confirm these predictions experimentally, we fabricated waveguide arrays with the zigzag geometry and required waveguide bending. Our samples contain 31 waveguides (16 in the bottom row and 15 in the top row). The length of the samples is  $L = 100 \text{ mm}$  and the waveguide spacing is  $d = 26 \mu\text{m}$ . The curved sample contains one full bending period. In order to visualize the light evolution which occurs inside the zigzag lattice between the bending periods, we employ a special fluorescence microscopy technique [37]. For the fabrication of the waveguides, we use fused silica with a high content of hydroxide. This leads to the formation of color centers in the waveguides during the laser-writing process. These color centers become excited when we launch the laser beam at the wavelength  $\lambda = 633 \text{ nm}$  into the waveguides, and images of the light propagation are recorded

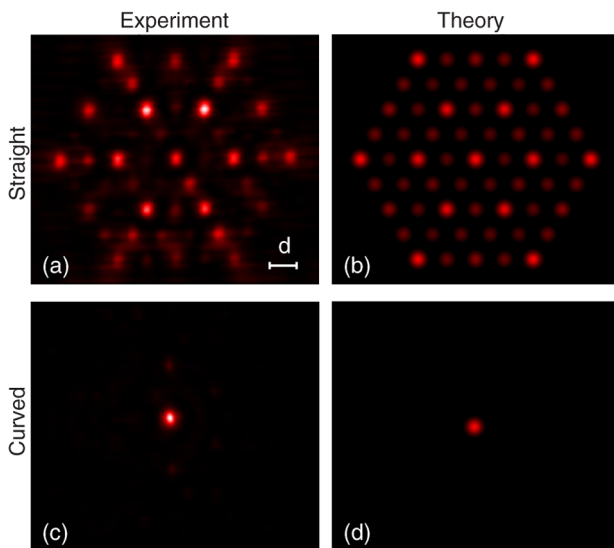


FIG. 2 (color online). (a) Experimentally measured and (b) numerically calculated output beam profiles for the hexagonal lattice created by straight waveguides. (c) Experimentally measured and (d) numerically calculated output beam profiles for the hexagonal lattice created by periodically curved waveguides.

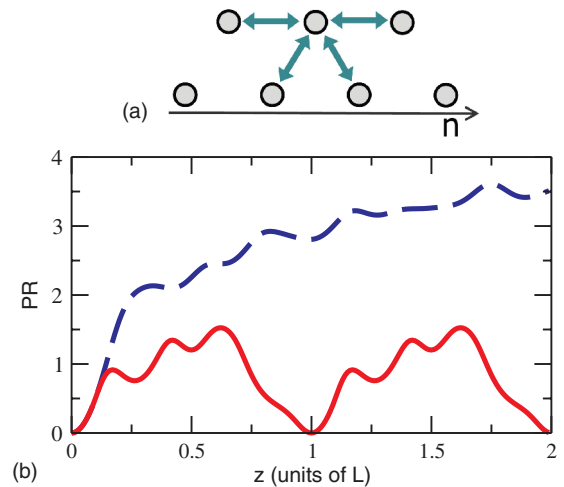


FIG. 3 (color online). (a) Sketch of the couplings in a zigzag array. (b) Numerically calculated participation ratios for the straight (dashed) and periodically curved (solid) waveguide arrays. Lattice parameters match the experiments in Fig. 4.



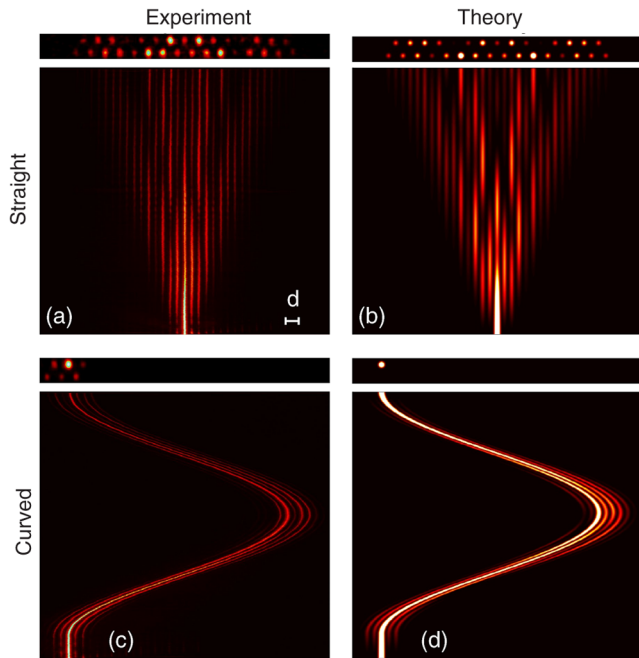


FIG. 4 (color online). (a) Experimentally measured output beam profiles (top) and fluorescent images of beam propagation (bottom) for the straight waveguide array. (b) Numerically calculated output beam profiles (top) and beam propagation (bottom) for the lattice created by straight waveguides. (c),(d) Same as (a) and (b) but for the periodically curved waveguides.

onto a CCD camera from the top of the sample [Figs. 4(a) and 4(c)]. In our experiments, light is coupled to the central waveguide in the top row of the zigzag array [Fig. 4].

In Figs. 4(a) and 4(c) experimentally recorded fluorescent images of the beam propagation inside the arrays are shown together with the measured output intensity distributions. Clearly, in the straight array the light field broadens significantly during propagation [Fig. 4(a)]. By matching the numerical simulations of Eq. (4) with the measured diffraction pattern at the output of the straight array [cf. Figure 4(a) and 4(b)] we find the value of the coupling coefficient to be  $C = 0.026 \text{ mm}^{-1}$ . In contrast, in the curved sample in the regime of dynamic localization, the light field initially broadens but then it refocuses again into the excited waveguide at the output of the array after the propagation over one full bending period [Fig. 4(c)], in excellent agreement with the corresponding numerical computations [Fig. 4(d)].

In conclusion, we have presented the first experimental observation of two-dimensional DL effect realized in modulated hexagonal photonic lattices laser written in fused silica. We have demonstrated that the DL effect in hexagonal lattices can be related to the light localization in quasi-one-dimensional zigzag waveguide arrays with the next-nearest-neighboring coupling. In the context of optics, our experiment provides a demonstration of full two-dimensional diffraction management based on the concept of the DL effect.

The authors acknowledge support by the Australian Research Council (Discovery and Center of Excellence programs), the Deutsche Forschungsgemeinschaft (Research Unit 532 and Leibniz program), the German Academy of Science Leopoldina (Grant No. LPDS 2009-13), and the Italian MIUR (Grant No. PRIN-2008-YCAAK).

- [1] S. Longhi, *Laser Photon. Rev.* **3**, 243 (2009).
- [2] P. Biagioni *et al.*, *Opt. Express* **16**, 3762 (2008).
- [3] G. Della Valle *et al.*, *Phys. Rev. Lett.* **98**, 263601 (2007).
- [4] M. Ornigotti *et al.*, *J. Phys. B* **41**, 085402 (2008).
- [5] F. Dreisow *et al.*, *Phys. Rev. Lett.* **101**, 143602 (2008).
- [6] N. Malkova *et al.*, *Opt. Lett.* **34**, 1633 (2009).
- [7] A. Szameit *et al.*, *Phys. Rev. Lett.* **101**, 203902 (2008).
- [8] S. John, *Phys. Rev. Lett.* **53**, 2169 (1984).
- [9] M. P. Van Albada and A. Lagendijk, *Phys. Rev. Lett.* **55**, 2692 (1985).
- [10] P. E. Wolf and G. Maret, *Phys. Rev. Lett.* **55**, 2696 (1985).
- [11] D. Wiersma, P. Bartolini, A. Lagendijk, and R. Righini, *Nature (London)* **390**, 671 (1997).
- [12] Y. Lahini *et al.*, *Phys. Rev. Lett.* **100**, 013906 (2008).
- [13] T. Schwartz, G. Bartal, S. Fishman, and M. Segev, *Nature (London)* **446**, 52 (2007).
- [14] T. Pertsch *et al.*, *Phys. Rev. Lett.* **83**, 4752 (1999).
- [15] R. Morandotti *et al.*, *Phys. Rev. Lett.* **83**, 4756 (1999).
- [16] H. Trompeter *et al.*, *Phys. Rev. Lett.* **96**, 053903 (2006).
- [17] H. Trompeter *et al.*, *Phys. Rev. Lett.* **96**, 023901 (2006).
- [18] A. Joushaghani *et al.*, *Phys. Rev. Lett.* **103**, 143903 (2009).
- [19] S. Longhi *et al.*, *Phys. Rev. Lett.* **96**, 243901 (2006).
- [20] R. Iyer *et al.*, *Opt. Express* **15**, 3212 (2007).
- [21] B. P. Anderson and M. A. Kasevich, *Science* **282**, 1686 (1998).
- [22] M. B. Dahan *et al.*, *Phys. Rev. Lett.* **76**, 4508 (1996).
- [23] H. Sanchis-Alepuz, Y. A. Kosevich, and J. Sánchez-Dehesa, *Phys. Rev. Lett.* **98**, 134301 (2007).
- [24] D. H. Dunlap and V. M. Kenkre, *Phys. Rev. B* **34**, 3625 (1986).
- [25] M. Holthaus, *Phys. Rev. Lett.* **69**, 351 (1992).
- [26] M. M. Dignam and C. M. de Sterke, *Phys. Rev. Lett.* **88**, 046806 (2002).
- [27] S. Longhi and K. Staliunas, *Opt. Commun.* **281**, 4343 (2008).
- [28] S. Fishman, D. R. Gempel, and R. E. Prange, *Phys. Rev. Lett.* **49**, 509 (1982).
- [29] K. W. Madison *et al.*, *Phys. Rev. Lett.* **81**, 5093 (1998).
- [30] A. Eckardt *et al.*, *Phys. Rev. A* **79**, 013611 (2009).
- [31] I. L. Garanovich *et al.*, *Opt. Express* **15**, 9737 (2007).
- [32] A. Szameit *et al.*, *Nature Phys.* **5**, 271 (2009).
- [33] A. Zenesini *et al.*, *Phys. Rev. Lett.* **102**, 100403 (2009).
- [34] S. Nolte, M. Will, J. Burghoff, and A. Tuennermann, *Appl. Phys. A* **77**, 109 (2003).
- [35] N. K. Efremidis and D. N. Christodoulides, *Phys. Rev. E* **65**, 056607 (2002).
- [36] F. Dreisow *et al.*, *Opt. Lett.* **33**, 2689 (2008).
- [37] A. Szameit *et al.*, *Appl. Phys. Lett.* **90**, 241113 (2007).